

**Variability of South American Convective Cloud Systems and Tropospheric Circulation  
during January-March 1998 and 1999**

*Rosana Nieto Ferreira* <sup>\*1</sup>, *Thomas M. Rickenbach* <sup>2</sup>, *Dirceu L. Herdies* <sup>1,3</sup>, and *Leila M. V.  
Carvalho* <sup>4</sup>

<sup>1</sup> Goddard Earth Sciences and Technology Center,  
University of Maryland, Baltimore County (UMBC)  
NASA Seasonal to Interannual Prediction Project GSFC  
Greenbelt, MD, USA

<sup>2</sup> NASA GSFC Data Assimilation Office, Greenbelt, MD, USA.  
(on leave from Centro de Previsão de Tempo e Estudos Climáticos, Instituto de  
Pesquisas Espaciais, São José dos Campos, Brazil).

<sup>3</sup> Joint Center for Earth Systems Technology (UMBC)  
NASA GSFC Mesoscale Processes Branch, Greenbelt, MD, USA

<sup>4</sup> Institute for Computational Earth System Sciences  
University of California, Santa Barbara, CA, USA  
(on leave from Departamento de Ciências Atmosféricas, Universidade de São  
Paulo, São Paulo, Brazil).

*Accepted in September 2002*

\*Corresponding Author Address: Rosana Nieto Ferreira, NASA GSFC, Code 913, Greenbelt,  
Maryland 20771 USA. Email: [ferreira@janus.gsfc.nasa.gov](mailto:ferreira@janus.gsfc.nasa.gov)

## Abstract

A comparison of the submonthly variability of atmospheric circulation and organization of convection in South America during January-March of 1998 (JFM98) and January-March of 1999 (JFM99) is presented. According to the National Centers for Environmental Prediction reanalysis, the South American low-level jet (SALLJ) was about twice as strong during January-March (JFM) of the 1998 El Niño episode than during JFM of the 1999 La Niña episode. The difference in SALLJ strength between these two years translated into stronger transport of moist tropical air into the subtropics during JFM98 than during JFM99. An objective tracking technique was used to identify large, long-lived convective cloud systems in infrared imagery. The stronger SALLJ was accompanied by larger and more numerous long-lived convective cloud systems and nearly twice as much rainfall in subtropical South America (parts of Southern Brazil, Uruguay, and Argentina) during JFM98 than during JFM99.

The difference between JFM98 and JFM99 SALLJ strength in Bolivia is in part explained by submonthly variability associated with the South Atlantic Convergence Zone (SACZ). Periods when the SACZ is present are marked by southerly or weak northerly winds in Bolivia. The South Atlantic Convergence Zone was more prominent during JFM99 than during JFM98 contributing to a weaker SALLJ during JFM99. Large, long-lived convective cloud systems in subtropical South America tended to occur during times when the SACZ was absent and the SALLJ was strong over Bolivia. Interannual variability associated with the El Niño-Southern Oscillation also contributed to the observed interannual variability of the SALLJ in Bolivia.

In the tropical portions of South America nearly six times more large, long-lived convective cloud systems were observed during JFM99 than during JFM98. This was accompanied by more plentiful precipitation in portions of the Amazon basin and in the Bolivian

Altiplano during JFM99 than during JFM98. Interannual variability associated with the El Niño-Southern Oscillation was an important contributor to the observed convective cloud system and precipitation differences in tropical South America.

## 1. Introduction

The long, narrow, low-level northerly wind current that flows to the east of the Andes mountains year round is known as the South American low-level jet (SALLJ, e.g., Nogues-Paegle and Mo 1997; Saulo et al. 2000). The SALLJ supplies the warm, moist tropical air that fuels convection and precipitation in the subtropical plains of South America (Saulo et al. 2000). The variability of precipitation in the subtropical plains of South America is therefore closely tied to the variability of the SALLJ. The SALLJ is in turn modulated by the El Niño -Southern Oscillation (ENSO) on interannual timescales (Zhou and Lau 2001), frontal passages and the South Atlantic convergence zone (SACZ) on submonthly timescales, and boundary layer dynamics on diurnal timescales. A preliminary study of the spatial structure and diurnal variability of the SALLJ is presented in Saulo et al. (2000). This paper focuses on the submonthly variability of the SALLJ and South American convection during January-March of the 1998 El Niño and January-March of the 1999 La Niña episodes.

On timescales of about a week, frontal systems passing through South America modulate the intensity and location of the SALLJ. Along the eastern slope of the Andes, baroclinic waves produce strong intrusions of cold air into the tropics that organize equatorward propagating synoptic scale bands of deep convection along the frontal boundary (Kousky 1985; Garreaud 2000). Ahead of the frontal system, low-level northwesterly flow extends from the tropics into midlatitudes contributing to a strong, well-defined SALLJ. In the wake of the frontal system, low-level southerly flow prevails and the SALLJ along the eastern slope of the Andes is weakened or absent.

The SACZ contributes to the modulation of the SALLJ on submonthly timescales (Seluchi and Marengo 2000). The SACZ is a northwest-southeast oriented stationary region of

enhanced convection that extends southeastward from the ITCZ convection anchored over the Amazon region into the South Atlantic Ocean. Each individual SACZ episode is composed of one or several midlatitude cold fronts that intrude into the subtropics and tropics, becoming stationary for a few days over southeastern Brazil. The SACZ is part of a well-known dipole pattern of submonthly variability of precipitation and circulation over South America (Casarin and Kousky 1986; Nogues-Paegle and Mo 1997; Liebmann et al. 1999; Nogues-Paegle et al. 2000). In this dipole pattern tropical air flows into the subtropics at two preferred longitudes. When the SACZ is absent, the SALLJ is located along the eastern foothills of the Andes Mountains, in Bolivia, carrying tropical moisture to fuel convection and precipitation in the Plata River Basin. When the SACZ is present the SALLJ is displaced eastward, diverting the tropical moisture flux away from the Plata River Basin and toward southeastern Brazil, along the stationary frontal zone (Herdies et al 2002; Rickenbach et al. 2002). In a study that encompassed eight southern summers, Sugahara et al. (1994) found that in days when the SALLJ is strong in Bolivia convection is intense in subtropical South America and weak in the SACZ region. They also found no modulation of Amazon convection by the strength of the SALLJ in Bolivia.

On interannual timescales, ENSO is the most important coupled ocean-atmosphere phenomenon to produce variability of South American precipitation and circulation patterns. Among the most consistent ENSO related precipitation anomalies in the Americas is the tendency for decreased precipitation during July of an El Niño year through March of the following year in northern Brazil, Suriname, Guiana and French Guiana, and Venezuela (Ropelewski and Halpert 1987; Lau and Sheu 1988). Coastal areas of Peru and Ecuador receive more rainfall than normal during El Niño years and less rainfall than normal during La Niña years (Aceituno 1988). In subtropical South America, the strongest positive precipitation anomalies occur during the austral spring of the year of the warm event (e.g., Lau and Sheu 1988; Pisciottano et al. 1994; Grimm et al. 2000). Negative precipitation anomalies prevail in subtropical South America during the

austral spring of a cold event year. ENSO precipitation anomalies in subtropical South America tend to weaken, and in some cases reverse, during the austral summer of the following year (Pisciottano et al. 1994; Grimm et al. 2000). While the tropical response to ENSO SST anomalies is dominated by atmospheric overturning in displaced Hadley and Walker cells (e.g., Trenberth et al. 1998), the extratropical response to ENSO SST anomalies occurs indirectly, through teleconnections. The precipitation and latent heating anomalies caused by ENSO tropical SST anomalies alter the forcing of large-scale Rossby waves that propagate into the extratropics producing, for instance, changes in extratropical storm tracks (e.g., Trenberth et al. 1998). Ultimately, the extratropical response to SST anomalies such as ENSO-related anomalies is less robust and predictable than the tropical response due to the chaotic nature of extratropical circulations such as transient baroclinic waves, fronts, and SACZ (e.g., Shukla et al. 2000).

Much of the growing season rainfall in the Plata River Basin is produced by large mesoscale precipitation systems. The precipitation produced by these systems benefits agriculture and hydroelectric power production in subtropical South America, but can also cause severe floods in major metropolitan areas (Torres and Nicolini, 1999). Mesoscale convective complexes (MCCs; Maddox 1980) are a well-studied subset of mesoscale precipitation systems characterized by their large size and longevity. The term MCC is an infrared satellite image-based definition of cloudiness that was coined by Maddox (1980) to classify the mesoscale systems that produce copious rainfall over the North American Great Plains during spring and summer. These systems display a nearly circular cold-cloud shield in infrared (IR) satellite imagery and produce heavy rainfall in many, mostly continental regions of the world including the Plata River Basin (Velasco and Fritsch 1987; Laing and Fritsch 1997). Most MCCs occur over land regions situated on the lee side of major topographic features and downstream from a low-level jet that brings a continuous supply of warm-moist tropical air to feed the convection (Maddox 1983; Laing and Fritsch 1997). In that sense, the Plata River Basin is a favorable region for the occurrence of

MCCs because it is located on the lee side of the Andes Mountains and downstream of the SALLJ which supplies warm and moist air from the Amazon Basin to feed the convection. Velasco and Fritsch (1987) used a two-year IR imagery dataset to document MCCs in the Americas and Eastern Pacific Ocean. In the tropical portions of their domain they documented the presence of MCCs in the Eastern Pacific Ocean, and in Colombia and Paraguay. In subtropical South America they documented large ( $5 \times 10^5$  km<sup>2</sup> average cold cloud shield), long-lived (mean duration of 11 hours), predominantly nocturnal MCCs (maximum cold cloud shields between 2 and 6 am local time), with a maximum frequency of occurrence during November through January.

MCCs have been studied extensively because their large circular, long-lived cloud shields are easily identified in IR satellite imagery, and their impact on the ambient large-scale flow is measurable by standard synoptic radiosonde networks (Maddox 1983). However, by focusing exclusively on MCCs it is likely that a large fraction of convective system variability will be missed. For example, Laing et al. (1999) reported that MCCs account for only 22 percent of wet season rainfall in the African Sahel and Fritsch et al. (1986) reported that 30 to 70 percent of summertime rainfall in the U. S. Great Plains is associated with MCCs. For this reason, Anderson and Arritt (1998) relaxed the most restrictive MCC criterion, that is, a nearly circular cloud shield, to include all large, long-lived convective cloud systems in the U. S. Great Plains. They found that this nearly tripled their convective system population.

In order to better understand the observed differences in South American atmospheric circulation and precipitation patterns between January-March 1998 (JFM98) and January-March 1999 (JFM99) we study the relationship between the SALLJ, the SACZ, and the organization of convection in South America on submonthly timescales during the two seasons. This work is based on a census of large, long-lived convective cloud systems (LLCS) for sub-regions in South

America using geostationary IR satellite imagery. This census therefore includes not only MCCs, but also large, long-lived convective systems with non-circular cloud shields, so as to capture a larger percentage of rainfall producing events.

This paper is organized as follows. Section 2 discusses a convective system objective tracking technique that is applied to three-hourly IR satellite imagery in order to characterize the temporal and spatial distribution of LLCS in South America. In section 3, the differences in LLCS populations over South America during JFM98 and JFM99 are studied within the context of the observed interannual variability of the atmospheric circulation given by the National Centers for Environmental Prediction (NCEP) reanalysis. In section 4, PACS-SONET (Pan-American Climate Studies Sounding Network) pilot balloon observations at Santa Cruz and Trinidad, Bolivia, are used to validate NCEP reanalysis low-level meridional winds for the study of submonthly variability of the SALLJ and LLCS. A summary of the results is presented in Section 5.

## **2. Convective system IR tracking technique**

A three-hourly global geostationary IR data set (14-km resolution) for JFM98 and JFM99 was obtained from the National Air and Space Administration's Global Hydrology Resource Center (NASA/GHRC) in Huntsville, Alabama. Previous studies (e.g. Laing and Fritsch 1997) have found that a three or even six hourly IR image interval is sufficient to characterize the seasonal MCC distribution and frequency in various regions around the world. Since our goal is to identify the approximate location, duration, and size of LLCS, a three-hourly IR image interval was considered adequate. These images were remapped by GHRC to a Mercator projection, making it possible to navigate them with good accuracy. We extracted a subset of the global images over South America, and applied a conversion from IR count to brightness temperature

used for the GOES-8 satellite. IR images for the periods between 1-4 and 7-9 January 1999 were missing.

Convective cloud systems were identified and tracked in consecutive IR images with the use of the Maximum Spatial Correlation Tracking Technique (MASCOTTE) (Carvalho and Jones 2001). In MASCOTTE, convective cloud systems are tracked with the assumption that the spatial correlation between regions defined by a given convective cloud system in consecutive images remains above a certain threshold. The methodology for identification of convective cloud systems and determination of the evolution and structural properties of its cloud shield using IR images is briefly discussed below. For more information such tracking techniques the reader is referred to Carvalho and Jones (2001), and Machado et al. (1998).

Individual convective cloud systems are defined as contiguous regions with brightness temperature ( $T_b$ ) colder than 220 K in the GOES (Geostationary Operational Environmental Satellite) IR images. While a threshold of 235 K for  $T_b$  has been used to identify structural properties of convective cloud systems in previous studies of MCCs (e.g., Maddox 1980; Velasco and Fritsch 1987), a careful examination of the IR images identified numerous problems with the use of the 235 K threshold. In the images used in this study, the 235 K contour often covered very large areas, many times an entire front or large areas of multiple convective cloud systems. The splitting, merging, and loss of continuity of the systems defined by the 235 K contour also caused the statistics produced by MASCOTTE using that threshold to be of little value. The MASCOTTE tracks were much improved with the use of the 220 K threshold. McAnelly and Cotton (1989) also modified Maddox's (1983) MCC identification threshold to use the 220 K brightness temperature contour in their study of MCC lifecycle and rainfall production over the U. S. Great Plains. As a justification for changing Maddox's temperature threshold they cite the fact that most rainfall is associated with colder cloud shields in addition to the problems discussed

above. The choice of a threshold value is in fact quite arbitrary and not based on any physical property of convective cloud systems. Moreover, it is well recognized that defining convective cloud systems by the contiguous cloud shield may obscure important details of the mesoscale organization and evolution of the underlying precipitation (Rickenbach 1999). An example of that is the presence of multiple precipitation systems under a common cloud shield.

In order to emphasize the modulation of convective cloud systems with longer life cycles, we consider systems with an equivalent radius ( $R = \sqrt{A/\pi}$ , where A is the area of the convective cloud system) of at least 100 km. A given convective cloud system lasts while its  $T_b$  is lower than 220 K, R is greater than 100 km, and while the spatial correlation between its IR cloud shield in two consecutive images remains greater than 0.3. The spatial correlation threshold of 0.3 was selected empirically after extensive examination of cloud system lifecycles produced by MASCOTTE (Carvalho and Jones 2001). MASCOTTE calculates various properties of the convective system cloud shield such as its center of gravity, horizontal area, and eccentricity (defined as the ratio of minor to major axes).

### **3 Convective cloud systems and atmospheric circulation during JFM98 and JFM99**

In this section we present the results obtained from the objective convective system IR tracking technique and relate them to the observed precipitation and tropospheric circulation patterns during the two contrasting ENSO seasons of JFM98 and JFM99.

#### **a. Observed precipitation and atmospheric circulation**

The mean observed precipitation and winds over South America and surrounding oceans during a neutral ENSO JFM are shown in Figs. 1c and 2c. The Xie-Arkin merged precipitation dataset is used to quantify precipitation in South America during JFM98 and JFM99. This global monthly precipitation dataset has  $2.5^\circ$  horizontal resolution and is based on gauge observations, satellite estimates, and numerical weather predictions (Xie and Arkin 1997). Data from the  $2.5^\circ$  horizontal resolution NCEP reanalysis is also shown. During JFM the Atlantic and Eastern Pacific Intertropical Convergence Zones (ITCZs) are weakest and located at their southernmost position just north of the Equator (Zhou and Lau 2001). In a neutral ENSO year (Fig. 1c), JFM precipitation in excess of  $9 \text{ mm day}^{-1}$  occurs throughout the Amazon basin with a maximum of 12 to  $15 \text{ mm day}^{-1}$  at the mouth of the Amazon river. Over the SACZ, precipitation in excess of  $6 \text{ mm day}^{-1}$  is observed. Subtropical South America (or SSA, which for the purposes of this study is defined as southern Brazil, Uruguay, Paraguay, and northern Argentina) receives over  $3 \text{ mm day}^{-1}$  of precipitation during a neutral JFM. The mean observed summertime low-level flow over tropical South America is dominated by the circulation around the South Atlantic subtropical high (Fig. 1c). Easterly winds flow from the equatorial Atlantic into the continent and become channeled southward by the Andes Mountains into the SALLJ. The observed mean summertime upper-level circulation over South America (Fig. 2c) is characterized by the presence of a prominent anticyclone centered over Bolivia (also known as the Bolivian high), the subtropical jet, and a trough over Northeast Brazil. Upward vertical velocities prevail over the Amazon basin, SACZ region and over the Atlantic ITCZ (Fig. 2c). The good consistency between regions of upward vertical velocity in the NCEP reanalysis and regions of precipitation in the Xie-Arkin dataset attest to the quality of the NCEP reanalysis.

Sharply contrasting Southern Oscillation conditions prevailed during JFM98 and JFM99. While during JFM98 one of the strongest El Niño episodes on record was under way in the

Pacific Ocean (Wolter and Timlin, 1998), strong La Niña conditions prevailed in the Pacific Ocean during JFM99. Figures 1a,b and 2a,b show the Xie-Arkin precipitation and NCEP wind and vertical velocity anomalies for JFM98 and JFM99. Anomalies were computed with respect to the JFM mean for neutral ENSO years.

ENSO affects tropical South America by producing zonal shifts of the Walker circulation in the Pacific-South American sector (e.g., Gill 1980; Gill and Rasmusson 1983). For instance, during JFM98 warm equatorial SST and enhanced precipitation were found eastward of their normal position in the Pacific Ocean. This eastward shift of the precipitation in the Pacific Ocean (Fig. 1a) produced an eastward shift of the Walker circulation with low-level equatorial westerly anomalies in the eastern Pacific and enhanced low-level equatorial easterlies over South America and the Atlantic Ocean (Fig. 1a). The upper-level circulation is in the opposite sense (Fig. 2a). Upward motion occurred in the eastern Pacific where precipitation was increased and subsidence occurred over tropical South America and the Atlantic ITCZ, suppressing precipitation in those regions (Fig. 2; Zhou and Lau 2001). While JFM98 had precipitation about 20 percent below average in the Atlantic ITCZ and Amazon basin (Fig. 1a,c), JFM99 had rainfall over 30 percent above average in the Western Amazon basin and in the Atlantic ITCZ (Fig. 1b,c). The Bolivian Altiplano received nearly 30 percent less rainfall in JFM98 than during a neutral ENSO year (Fig. 1b,c). Both years had below average precipitation in the SACZ region.

The SALLJ was about twice as strong during JFM of the 1998 El Niño episode than during JFM of the 1999 La Niña episode (Fig. 1). This led to strong vertically integrated northerly moisture fluxes toward the SSA region (Fig. 3a) and contributed to up to twice as much precipitation during JFM98 than during JFM99 in the SSA (Fig. 1a,b). The stronger low-level trade-wind easterlies in the Amazon basin during JFM98 may have contributed to a stronger SALLJ during JFM98 than during JFM99. Zhou and Lau (2001) found a statistically significant

positive correlation between the tropical Eastern Pacific SST and the strength of the SALLJ. They argue that the eastward shift of equatorial Pacific precipitation during an El Niño year causes a strengthening of the South Atlantic subtropical high which is in turn associated with stronger equatorial Atlantic easterlies and a stronger SALLJ.

## **b. Convective system IR statistics**

In order to isolate the largest, longest-lived convective cloud systems, or LLCS, a subset of the convective cloud systems tracked by MASCOTTE was selected based on their size, duration, and eccentricity. Hereafter, only those systems that obeyed the following criteria are considered: a) area covered by the 220 K contour greater than  $2 \times 10^5 \text{ km}^2$ , b) area covered by the 210 K contour greater than  $1 \times 10^4 \text{ km}^2$ , c) eccentricity greater than 0.2, and d) duration of at least 3 consecutive images (or at least 6 hours). As discussed in the introduction, the eccentricity criterion in the MCC definition was relaxed so as to include all systems with large, long-lived cloud shields, without restricting the sample to only those systems with circular cloud shields. From the more than two thousand systems originally tracked by MASCOTTE, only 135 obeyed the above criteria and will be studied below.

The JFM98 and JFM99 spatial distributions of LLCS at the time when they were largest are shown in Fig. 4. The study region was divided into the three regions of interest labeled as SSA, TROPICS, and SACZ in Fig. 4. The SACZ and SSA regions defined here were based on the two regions of strongest subseasonal variance of OLR in South America (Fig. 3a of Liebmann et al. 1999). These regions are at the opposite extremes of the prominent dipole pattern of precipitation in South America that links enhanced precipitation in the SACZ region with suppressed precipitation in the SSA region, and vice-versa (e.g., Casarin and Kousky 1986; Nogues-Paegle and Mo 1997). The remainder of South America and the Tropical Atlantic are

defined as TROPICS. The SSA and TROPICS regions are part of another dipole of precipitation in South America associated with ENSO variability (e.g. Zhou and Lau 2001). Therefore the definition of the SSA, SACZ, and TROPICS regions is based on the main patterns of submonthly to interannual variability that are the focus of this study.

Table 1 shows the number of LLCS, their mean duration and mean maximum area categorized by year and region. Although LLCS are tracked by MASCOTTE using the 220 K contour, the 210 K threshold may be more closely related to the dynamically active portion of the system. The LLCS in Fig. 4 and Table 1 are characterized by the center of the 210 K contour and by the eccentricity and maximum area of the 220 K contour. Overall, there were half as many LLCS in South America during JFM98 as there were in JFM99. While the majority of the South American LLCS during JFM98 occurred in the SSA region, the majority of LLCS in JFM99 occurred in the TROPICS region. In the SSA region, there were fifty percent more LLCS during JFM98 (El Niño) than during JFM99 (La Niña). Velasco and Fritch (1987) found a similar ENSO modulation for MCCs in the SSA region, with twice as many MCCs during the 1982-1983 El Niño than during the 1981-1982 non-El Niño year. Besides being more numerous, the JFM98 SSA region systems had mean maximum area about 40 percent larger than those during JFM99. In the TROPICS region, there were about six times more systems during JFM99 than during JFM98. The number of LLCS in the SACZ region in JFM99 was twice that of JFM98.

While a detailed study of the rainfall associated with the LLCS is beyond the scope of this study, previous studies have shown that these systems produce large amounts of rainfall (e.g., Fritsch et al. 1986; Velasco and Fritsch 1987; Torres and Nicolini 1999). Hence, the increased precipitation in the SSA region during JFM98 (Fig. 1a) is consistent with the occurrence of more and larger LLCS. Likewise, the increased precipitation in the land portion of the TROPICS region (Fig. 1b) during JFM99 is consistent with the occurrence of more numerous LLCS during JFM99

than during JFM98. The good agreement between the results of the MASCOTTE convective system statistics and the mean Xie-Arkin precipitation is expected since the GOES IR imagery is one of the datasets used in the Xie-Arkin estimation of precipitation. The convective system statistics, however, produces information on the spatial organization (location and size) and temporal distribution (time of occurrence and duration) of precipitating events that is absent in the Xie-Arkin precipitation dataset.

Only 8 of the 135 LLCS in this study occurred over the Atlantic Ocean (Fig. 4). Although many frontal systems passed through the oceanic portions of the SACZ and SSA regions, only 5 of the oceanic convective cloud systems embedded in these frontal regions obeyed the necessary criteria for inclusion in this study. This is in part due to the fact that cloud shields of oceanic convective cloud systems were in general warmer and more elongated than those of convective cloud systems that occurred over land. In the Atlantic ITCZ region, only 3 convective cloud systems obeyed the criteria established for inclusion in this study.

A histogram of the time of day when LLCS of JFM98 and JFM99 reached their maximum cold cloud-shield area for each of the three study regions is shown in Fig. 5. In good agreement with previous studies (e.g., Anagnostou et al. 1999), most LLCS in the TROPICS and SACZ regions reached their maximum cold cloud-shield area in the late afternoon to early evening hours. In the SSA region most LLCS reached their maximum cold cloud-shield area in the nighttime to early morning hours, also in good agreement with previous studies (e.g., Velasco and Fritsch 1987).

In summary, we have shown that very different LLCS populations and large-scale circulation and precipitation patterns occurred over most of South America during JFM98 and JFM99. The tropospheric circulation during JFM98 included a stronger SALLJ and a stronger

upper-tropospheric subtropical westerly jet<sup>1</sup>, both of which have been shown in previous studies to favor the formation of large, long-lived convective cloud systems (e.g., Maddox 1980, Velasco and Fritsch 1987). Stronger rainfall in the SSA during JFM98 was consistent with more numerous and larger convective cloud systems during that year. Increased subsidence during the Niño year (Fig. 2a) is linked to a decreased number of LLCS and decreased precipitation in the Amazon basin when compared to the Niña year.

#### **4. Submonthly variability of the SALLJ and convective system statistics**

Due to the sparseness and intermittency of the South American radiosonde network, the structure and temporal variability of the SALLJ are not well known. During the Southern Hemisphere summers of 1998 and 1999, pilot balloon observations were made in Bolivia under the auspices of the PACS-SONET field campaign. Pilot balloon observations at Santa Cruz and Trinidad (Bolivia; see Fig. 4 for the location of these stations) are available for some portions of the study period. Note that Santa Cruz and Trinidad are located in the region where the SALLJ has maximum intensity (see Fig. 1c). The mean NCEP low-level jet intensity at 850 mb was about  $4 \text{ m s}^{-1}$  stronger during JFM98 than during JFM99 (Fig. 1). The pilot balloon observations at Trinidad and Santa Cruz were not assimilated by the NCEP reanalysis and therefore provide independent verification of the NCEP products. Figures 6 and 7 show timeseries of the observed 850 mb meridional wind at Santa Cruz and Trinidad along with the timeseries of meridional winds analyzed by the NCEP reanalysis at the model gridpoint that is closest to Santa Cruz. NCEP reanalysis meridional winds are plotted every six hours. Santa Cruz and Trinidad pilot balloon observations were available up to three times daily. Since the Santa Cruz pilot balloon

---

<sup>1</sup> Regions of enhanced upper level westerlies in the subtropics or midlatitudes are associated with strong surface temperature gradients and enhanced frontogenesis. In the summer season, fronts provide mechanisms that favor the occurrence of organized convective systems such as squall lines and mesoscale convective systems (Bluestein 1993).

dataset for JFM99 is very incomplete, we use the dataset collected at the nearby station of Trinidad during JFM99. Overall the NCEP reanalysis captures well the observed daily fluctuations of the meridional low-level wind in Santa Cruz and Trinidad during the period of this study. During JFM98, however, the NCEP reanalysis has a negative bias with respect to the JFM98 Santa Cruz pilot balloon observations resulting in what may be an unrealistically strong analyzed mean northerly jet in Bolivia during January and February of 1998. This bias does not occur in Trinidad during JFM99 and could reflect a deficiency of the NCEP reanalysis in resolving the details of the flow in a region like Santa Cruz, which is at the bottom of a steep incline that leads up to the Bolivian Plateau.

The Brazilian Space Agency's monthly climate bulletin, *Climanálise*, provides information on the passage of fronts in South America as well as on the status of the SACZ<sup>2</sup>. Thin solid lines at the bottom of Figs. 6a and 7a denote times when a frontal system was present anywhere along the Atlantic coast of South America. The low-level meridional wind signature of a frontal passage is marked by periods of northerly winds followed by southerly winds. Good examples are the frontal systems that occurred on 7-11 January 1998 and 10-15 February 1998. The latter became stationary over the coast of Rio de Janeiro between 12-16 February constituting the first SACZ episode of 1998. The grey rectangles at the bottom of Figs. 6a and 7a mark the presence of the SACZ. The SACZ episode of February of 1998 was associated with very strong low-level southerly winds in the Santa Cruz pilot balloon observations that lasted for a few days and reached  $30 \text{ m s}^{-1}$ . Note that not all fronts penetrate deep enough into lower latitudes to affect

---

<sup>2</sup> *Climanálise* uses the following criteria to define SACZ episodes:

- 1) Permanence of a northwest-southeast oriented band of cloudiness that extends from the Amazon basin to the Atlantic ocean for at least 4 days,
- 1) Presence of low-level moisture convergence in the aforementioned region that lasts for at least 4 days,
- 1) Presence of cold air to the south of the semi-stationary system,
- 1) Presence of a northwest-southeast oriented trough at 500 mb to the east of the Andes Mountains,
- 1) In the upper-levels, the Bolivian high is present, along with a trough in Northeast Brazil and anticyclonic vorticity above the semi-stationary cloud band.

stations in Bolivia. It is interesting to point out that while the February 1998 SACZ episode was produced by one frontal system, the SACZ episodes that occurred during January and February of 1999 were each produced by two or more fronts that became stationary somewhere in the southeastern coast of Brazil.

An analysis of the submonthly variability of the SALLJ and SACZ and their relationship to the presence of LLCS in SSA is now presented. The histograms in Figs. 6b and 7b show the timing of LLCS occurrence in the SSA and SACZ regions with respect to low-level meridional wind variability in Bolivia. The majority of LLCS in the SSA region occurred when there were strong low-level northerly winds in Bolivia. These strong bursts of low-level northerly winds carry into the SSA the tropical moisture that fuels the LLCS that occur in that region. Table 2 shows how the mean NCEP meridional low-level winds in Bolivia vary with LLCS and SACZ occurrence. It shows that LLCS occurred in SSA during periods of stronger low-level northerly winds in Bolivia, a result that is statistically significant at the 95 percent level according to a Student's *t*-test. According to Fig. 6, SACZ periods were marked by weak northerly or southerly winds in Bolivia and no LLCS in the SSA region. This is confirmed in Table 2, where it is shown that low-level northerly winds in Bolivia were fifty percent weaker during periods when the SACZ was present than during periods when the SACZ was absent. This result is also statistically significant to the 95 percent level according to a Student's *t*-test.

In summary, Figs. 6 and 7 and Table 2 show that in the absence of the SACZ there is a tendency for stronger low-level northerly winds in Bolivia and a larger number of LLCS in the SSA. During SACZ periods, the SALLJ tends to be displaced away from the Andes mountains cutting off the tropical moisture supply for the SSA region (e.g., Nogues-Paegle and Mo 1997; Seluchi and Marengo 2000; Herdies et al. 2002; Rickenbach et al. 2002). While the SACZ was present during 40 days in JFM99, it was present for only about 10 days in JFM98. The weaker

presence of the SACZ over South America during JFM98 than during JFM99 also contributed to a stronger SALLJ in Bolivia and stronger precipitation in the SSA during JFM98. Hence the interannual variability of the SALLJ and precipitation in the SSA region observed between JFM98 and JFM99 is in part explained in terms of the variability of the SACZ on submonthly timescales.

## **5. Conclusions**

An observational study of the January-March 1998-1999 differences in precipitation, atmospheric circulation and occurrence of large, long-lived convective cloud systems in South America was presented. Strongly contrasting Southern Oscillation conditions prevailed during JFM98 and JFM99. Whereas one of the strongest El Niño episodes on record was under way in the Pacific Ocean during JFM98, strong La Niña conditions prevailed in the Pacific Ocean during JFM 1999.

Much of the precipitation in the subtropical regions of South America is produced by large, long-lived convective cloud systems (e.g., Velasco and Fritsch 1987; Torres and Nicolini 1999). An objective tracking technique (Carvalho and Jones 2001) was used to identify these systems in IR imagery. Statistics were compiled on systems whose a) area covered by the 220 K contour was greater than  $2 \times 10^5$  km, b) area covered by the 210 K contour was greater than  $1 \times 10^4$  km, c) eccentricity was greater than 0.2, and d) lasted for at least 3 consecutive images (or at least 6 hours). Overall, twice as many LLCS were observed in South America during JFM99 than in JFM98. Moreover, while the majority of the South American LLCS during JFM98 occurred in the SSA region, the majority of LLCS in JFM99 occurred in the TROPICS region. In the SSA region, there were fifty percent more LLCS during JFM98 (El Niño) than during JFM99 (La Niña). During JFM98, LLCS in the SSA region had mean maximum area about 40 percent larger

than those during JFM99. The presence of larger and more numerous convective cloud systems in the SSA region during JFM98 is consistent with the nearly doubled rainfall observed in the SSA region during JFM98 than during JFM99.

In the TROPICS region, nearly six times more LLCS were observed during JFM99 than during JFM98. This was accompanied by more plentiful precipitation in the Amazon basin and in the Bolivian Altiplano during JFM99 than during JFM98. The suppressed precipitation in the TROPICS region during JFM98 was associated with enhanced subsidence associated with the characteristic eastward shift of the Pacific Walker circulation during El Niño episodes.

On submonthly timescales, the SACZ modulated the SALLJ and the occurrence of LLCS in SSA. During the portions of the study period when the SACZ was absent, there was a tendency for stronger low-level northerly winds in Bolivia (Herdies et al. 2002; Rickenbach et al. 2002) and a larger number of LLCS in subtropical South America (Sugahara et al. 1994). The SACZ was present during more than a month in JFM99 and for only a few days in JFM98, therefore contributing for the observed difference in SALLJ and SSA precipitation and LLCS formation between the two years.

On interannual timescales, ENSO modulated the strength of the SALLJ and the formation of LLCS in the TROPICS and SSA regions. According to the NCEP reanalysis, the SALLJ was about twice as strong during JFM of the 1998 Niño episode than during JFM of the 1999 Niña episode. This caused a stronger inflow of moist tropical air into subtropical South America (SSA) favoring the occurrence of larger and more numerous convective cloud systems and more plentiful precipitation in SSA. To the extent that trade winds over the Amazon basin are channeled southward by the Andes Mountains (e.g., Gandu and Geisler 1991; Seluchi and Marengo 2000), it is possible that the strengthened trade easterly winds across the Amazon basin

during JFM98 contributed to a stronger SALLJ. The presence of a stronger than normal subtropical jet during JFM98 may also have contributed to the formation of more LLCS in the SSA region during that year (consistent with the findings of Velasco and Fritsch 1987).

Both interannual variability associated with ENSO, and submonthly variability associated with the SACZ contributed to a stronger SALLJ in Bolivia, and to more numerous and larger convective cloud systems and enhanced precipitation in the SSA during JFM98. While previous studies have tied the intraseasonal variability of the SACZ to the variability of the South Pacific convergence zone through a Rossby wave-guide in the South Pacific Ocean (Nogues-Paegle and Mo 1997; Liebmann et al. 1999), the interannual variability of the SACZ remains to be assessed.

The LLCS included in this study do not produce all of the precipitation reported in the Xie-Arkin observations. Smaller, shorter-lived, more elongated, or systems with warmer cloud tops also contribute to the total rainfall. On the other hand, LLCS are relatively easy to track and have been shown by previous studies to be significant producers of rainfall. The details of the complex relationships between cloud shield size, duration, propagation, and cloud system precipitation (stratiform or convective) were beyond the scope of this study.

## **Acknowledgments**

This project was funded in part by grants from the NASA Large-scale Biosphere Atmosphere (LBA) Hydrology project, from the Tropical Rainfall Measuring Mission, and from FAPESP (Proc. 98/14414-0). Geostationary satellite data was obtained from NASA/GHRC at the Global Hydrology and Climate Center, Huntsville, Alabama, USA. DLH contributed to this work while in a visiting scientist position with Dr. Arlindo da Silva at NASA's Data Assimilation Office. DLH's contribution to this work is part of his PhD thesis dissertation at the University of São

Paulo, Brazil, under the advice of Dr. Maria Assunção Faus da Silva Dias. The authors gratefully acknowledge the insightful comments of two anonymous reviewers.

## References

- Aceituno, P., 1988: On the functioning of the Southern Oscillation in the South American sector, I, surface climate. *Mon. Wea. Rev.*, **116**, 505-525.
- Anagnostou, E. N., A. J. Negri, and R. F. Adler, 1999: A satellite infrared technique for diurnal rainfall variability studies. *J. Geophys. Res.*, **104**, D24, 31477-31488.
- Anderson, C. J. and R. W. Arritt, 1998: Mesoscale convective complexes and persistent elongated convective systems over the United States during 1992 and 1993. *Mon. Wea. Rev.*, **126**, 578-599.
- Bluestein, H. B., 1993: Synoptic-Dynamic Meteorology in Midlatitudes - Volume II: Observations and Theory of Weather Systems. *Oxford University Press*, 594 pp.
- Carvalho, L. M. V. and C. Jones, 2001: A satellite method to identify structural properties of mesoscale convective systems based on Maximum Spatial Correlation Tracking Technique (MASCOTTE). *J. Appl. Meteor.* 1683–1701.
- Casarin, D. P., and V. E. Kousky, 1986: Precipitation anomalies in southern Brazil and atmospheric circulation variability (Portuguese). *Rev. Bras. Meteor.*, **1**, 83-90.
- Climanálise, Boletim de monitoramento e análise climática, Vols. 13,14, numbers 1, 2. Available from *Centro de Previsão de Tempo e Estudos Climáticos, Rodovia Presidente Dutra, km*

240 SPRJ, 12630-000, Cachoeira Paulista - SP, Brasil, or on the web at <http://www.cptec.inpe.br/products/climanalise/capal.html>.

Fritsch, J. M., R. J. Kane, and C. R. Chelius, 1986: The contribution of mesoscale convective weather systems to the warm-season precipitation in the United States. *J. Clim. Appl. Meteor.*, **25**, 1333-1345.

Gandu, A. W., and J. E. Geisler, 1991: A primitive equations model study of the effect of topography on the summer circulation over tropical South America. *J. Atmos. Sci.*, **48**, 1822-1836.

Garreaud, R. D., 2000: Cold air intrusions over subtropical South America: mean structure and dynamics. *Mon. Wea. Rev.*, **128**, 2544-2559.

Gill, A. E., 1980: Some simple solutions for heat-induced tropical circulation. *Quart. J. R. Met. Soc.*, **106**, 447-462.

Gill, A. E., and E. M. Rasmusson, 1983: The 1982-83 climate anomaly in the equatorial Pacific. *Nature*, **306**, 229-234.

Grimm, A. M., V. R. Barros, and M E. Doyle, 2000: Climate variability in southern South America associated with El Niño and La Niña events. *J. Climate*, **13**, 35-58.

Herdies, D. L., A. Silva, M. A. F. Silva Dias, and R. Nieto Ferreira, 2002: The bi-modal pattern of the summer circulation over South America. *Submitted to the J. Geophys. Res.*

- Kousky, V. E., 1985: Atmospheric circulation changes associated with rainfall anomalies over tropical Brazil. *Mon. Wea. Rev.*, 113, 1951-1957.
- Laing, A. G., and J. M. Fritsch, 1997: The global population of mesoscale convective complexes. *Quart. J. Roy. Meteor. Soc.*, **123**, 389-405.
- Laing, A. G, J. M. Fritsch, and A. J. Negri, 1999: Contribution of mesoscale convective complexes to rainfall in Sahelian Africa: Estimates from geostationary infrared and passive microwave data. *J. Appl. Meteor.*, **38**, 957-964.
- Lau, K.-M and P. J. Sheu, 1988: Annual cycle, Quasi-Biennial Oscillation, and Southern Oscillation in global precipitation. *J. Geophys. Res.*, 93, 10975-10988.
- Liebmann, B., G. N. Kiladis, J. A. Marengo, T. Ambrizzi, and J. D. Glick, 1999: Submonthly variability over South America and the South Atlantic convergence zone. *J. Climate*, **12**, 1877-1891.
- Machado, W. B. Rossow, R. L. Guedes, and A. W. Walker, 1998: Life cycle variations of mesoscale convective systems over the Americas. *Mon. Wea. Rev.*, 126, 1630-1654.
- Maddox, R. A., 1980: Mesoscale convective complexes. *Bull. Am. Meteorol. Soc.*, **61**, 1374-1387.
- Maddox, R. A., 1983: Large-scale meteorological conditions associated with midlatitude, mesoscale convective complexes. *Mon. Wea. Rev.*, **111**, 1475-1493.

- McAnelly, R. L. and W. R. Cotton, 1989: The precipitation life cycle of mesoscale convective complexes over the United States. *Mon. Wea. Rev.*, **117**, 784-807.
- Nogues-Paegle, J., and K. C. Mo, 1997: Alternating wet and dry conditions over South America during summer. *Mon. Wea. Rev.*, **125**, 279-291.
- Nogues-Paegle, J. N., L. A. Byerle, and K. C. Mo, 2000: Intraseasonal modulation of South American summer precipitation. *Mon. Wea. Rev.*, **128**, 837-850.
- Pisciottano, G., A. Díaz, G. Cazes, and C. R. Mechoso, 1994: El Niño-Southern Oscillation impact on rainfall in Uruguay. *J. Climate*, **7**, 1286-1302.
- Rickenbach, T. M., 1999: Cloud-top evolution of tropical oceanic squall lines from radar reflectivity and infrared satellite data. *Mon. Wea. Rev.*, **127**, 2951-2976.
- Rickenbach, T. M., R. Nieto Ferreira, J. Halverson, D. L. Herdies, and M. A. F. Silva Dias, 2002: Modulation of convection in the southwestern Amazon basin by extratropical stationary fronts. *J. Geophys. Res.*, *In Press*.
- Ropelewski, C. F., and M. S. Halpert, 1987: Global and regional scale precipitation patterns associated with the el Niño/Southern Oscillation. *Mon. Wea. Rev.*, **115**, 1606-1626.
- Saulo, A. C., M. Nicolini, and S. C. Chou, 2000: Model characterization of the South American low-level flow during the 1997-1998 spring-summer season. *Clim. Dynamics*, **16**, 867-881.

- Seluchi, M. E., and J. A. Marengo, 2000: Tropical-midlatitude exchange of air masses during summer and winter in South America: climatic aspects and examples of intense events. *Int. J. Climatol.*, **20**, 1167-1190.
- Shukla, J., J. Anderson, D. Baumhefner, C. Brankivik, Y. Chang, E. Kalnay, L. Marx, T. Palmer, D. Paolino, J. Ploshay, S. Schubert, D. Straus, M. Suarez, and J. Tribbia, 2000: Dynamical seasonal prediction. *Bull. Amer. Meteor. Soc.*, **81**, 2593-2606.
- Sugahara, S., R. P. Rocha, and M. L. Rodrigues, 1994: Condições atmosféricas de grande escala associadas a jato de baixos níveis na América do Sul. Proceedings of the 8th Brazilian Meteorology Conference, Brazilian Meteorological Society, 573-577.
- Torres, J. C., and M. Nicolini, 1999: Analysis of a mesoscale convective system centred over the Río de la Plata. *Aust. Met. Mag.*, **48**, 261-272.
- Trenberth, K. E., G. W. Branstator, D. Karoly, A. Kumar, N.-C. Lau, and C. Ropelewski, 1998: Progress during TOGA in understanding and modeling global teleconnections associated with tropical sea surface temperatures. *J. Geophys. Res.*, **103**, 14291-14324.
- Velasco, I., and M. Fritsh, 1987: Mesoscale convective complexes in Americas. *J. Geophys. Res.*, **92**, 9591-9613.
- Wolter K., and M. S. Timlin, 1998: Measuring the strength of ENSO - how does 1997/98 rank? *Weather*, **53**, 315-324.

Xie, and Arkin, 1997: Global precipitation: A 17-year monthly analysis based on gauge observations, satellite, and numerical model outputs. *Bull. Amer. Met. Soc.*, **78**, 2539-2558.

Zhou, J., and W.-K. Lau, 2001: Principal modes of interannual and decadal variability of summer rainfall over South America. *Int. J. Climatol.*, **21**, 1623-1644.

		<i>TROPICS</i>	<i>SACZ</i>	<i>SSA</i>	<i>TOTAL</i>
<b>JFM98</b>	Number	10	8	26	44
	Mean Max. Area ( $10^5 \text{ km}^2$ )	10.6	9.4	10.8	10.5
<b>El Niño</b>	Mean Duration (h)	16	11	20	17
<b>JFM99</b>	Number	56	16	17	89
	Mean Max. Area ( $10^5 \text{ km}^2$ )	10.4	13	7.5	10.3
<b>La Niña</b>	Mean Duration (h)	15	17	18	16

Table 1: Number, maximum area of the 220K cloud shield, and duration of convective cloud systems tracked by MASCOTTE in JFM98 and JFM99 in the TROPICS, SACZ, and SSA regions.

	<b>SACZ</b>	<b>Non-SACZ</b>	<b>LLCS</b>	<b>No-LLCS</b>
$\bar{V}$	-3.6	-7.2	-9.6	-5.8
N	35	145	39	141

Table 2: Comparison of four-times daily NCEP reanalysis meridional winds in Bolivia during SACZ and non-SACZ periods, and during periods when LLCS occurred in the SSA versus periods when no LLCS occurred in the SSA.  $\bar{V}$  is the mean meridional wind for each period, and N is the number of days in each category.

## Figure Captions

Figure 1: Xie-Arkin (Xie and Arkin 1997) precipitation ( $\text{mm day}^{-1}$ ) and 850 mb NCEP winds ( $\text{m s}^{-1}$ ). a) 1998 anomalies, b) 1999 anomalies, and c) neutral. Anomalies in a) and b) are calculated with respect to a neutral ENSO composite in c). Neutral ENSO years were selected according to a Climate Prediction Center (CPC) table of seasonal conditions in the tropical Pacific Ocean. Averages in c) are for years in which no strong or moderate La Niña or El Niño was present during JFM according to the CPC (namely, 1979-1982, 1984-1986, 1988, 1990, 1991, 1993, 1994, 1996, 1997). ([http://www.cpc.ncep.noaa.gov/products/analysis\\_monitoring/ensostuff/ensoyears.html](http://www.cpc.ncep.noaa.gov/products/analysis_monitoring/ensostuff/ensoyears.html)). Contours are  $\pm 1$ ,  $\pm 2$ ,  $\pm 4$ ,  $\pm 8$   $\text{mm day}^{-1}$  in a) and b) and every 3  $\text{mm day}^{-1}$  in b). Dashed contours are negative, solid contours are positive, and the zero contour is not plotted.

Figure 2: Same as Fig. 1, but for the 200 mb NCEP winds ( $\text{m s}^{-1}$ ) and 500 mb NCEP vertical velocity ( $\text{Pa s}^{-1}$ ). Contours are every 0.01  $\text{Pa s}^{-1}$  in a) and b) and every 0.02  $\text{Pa s}^{-1}$  in c). Dashed contours are negative, solid contours are positive, and the zero contour is not plotted.

Figure 3: NCEP reanalysis vertically (850-200 mb) integrated moisture flux ( $\text{Kg m}^{-1} \text{s}^{-1}$  for a) JFM98 and b) JFM99.

Figure 4: Spatial distribution of LLCS tracked by MASCOTTE during a) JFM98 and b) JFM99. Circles denote the position and size of each convective system at the time of maximum area (measured as the central position of the 210 K contour and area defined by the 220 K

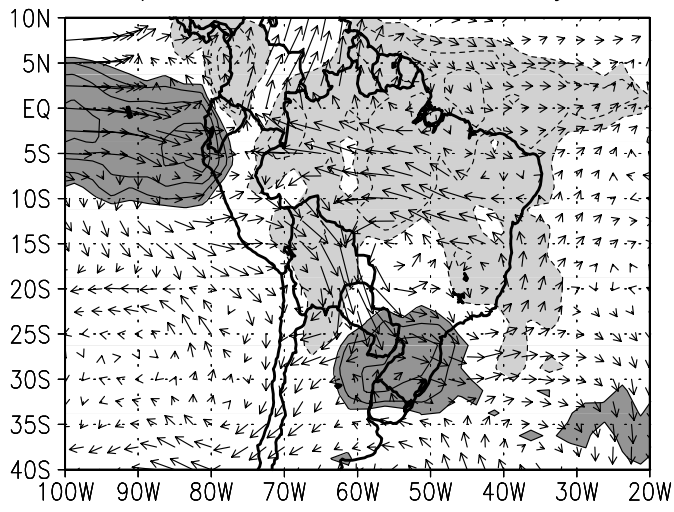
contour). The area of each circle is about a fifth of the area of the corresponding convective system.

Figure 5: Histogram of the time of day when all convective cloud systems that occurred during JFM98 and JFM99 reached their maximum cold cloud-shield area (measured as the area defined by the 220 K contour) for each of the three study regions. The SSA region Local Standard Time (LST) is 4 hours behind GMT time. The SACZ region LST is 3 to 4 hours behind GMT time. The TROPICS region LST is 3 to 5 hours behind GMT time.

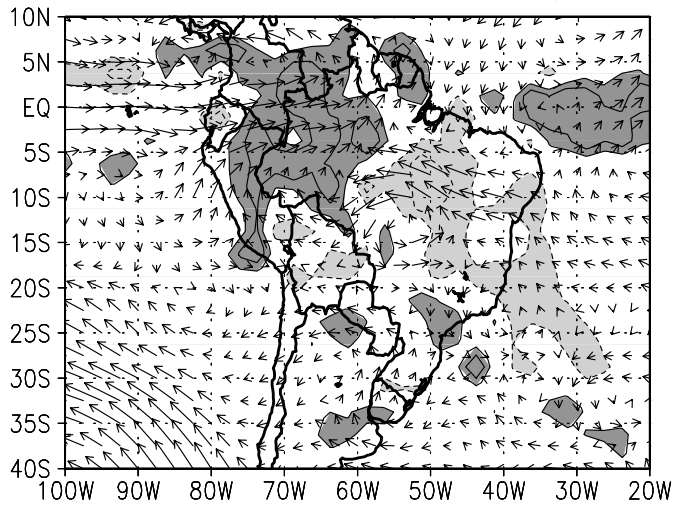
Figure 6: JFM98 submonthly variability of the low-level winds at Santa Cruz, Bolivia, as well as fronts, and SACZ episodes in South America, and convective cloud systems in the SSA and SACZ regions. a) Meridional component of the wind in Santa Cruz, Bolivia during JFM98. Asterisks linked by dashed lines denote pilot balloon observations (available up to three times daily). Solid lines denote four-times daily NCEP reanalysis data at the datapoint closest to Santa Cruz. Solid boxes and thin solid lines at the bottom of a) denote SACZ periods and frontal systems, respectively. b) histogram of the number of convective cloud systems that occurred in the SSA (dark grey) and SACZ regions (light grey).

Figure 7: Same as Fig. 5, but for Trinidad, Bolivia during JFM99.

a) 1998 Anomaly



b) 1999 Anomaly



c) Neutral

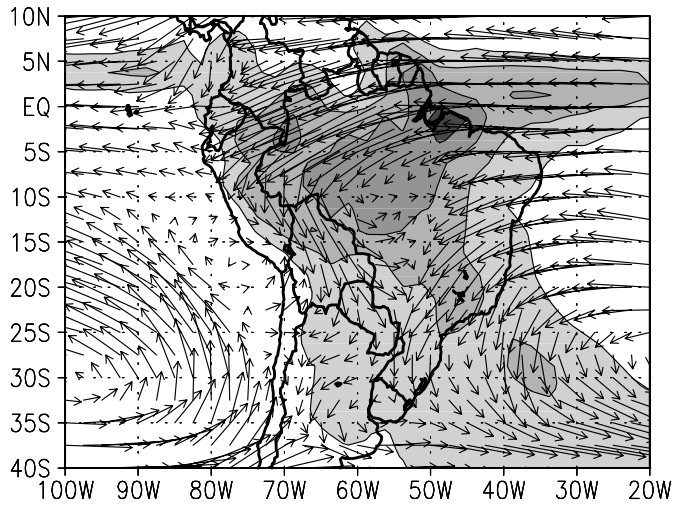
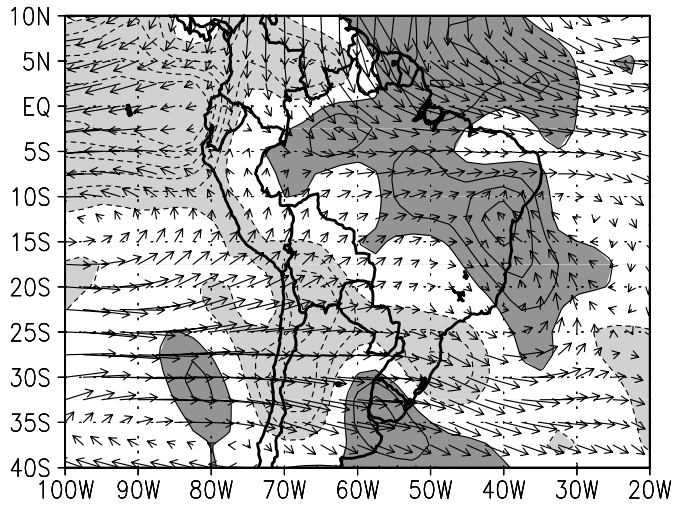


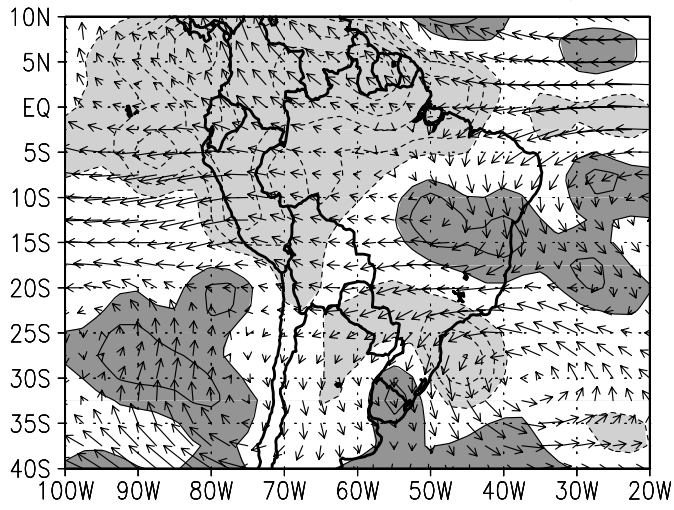
FIGURE 1

→  
10

a) 1998 Anomaly



b) 1999 Anomaly



c) Neutral

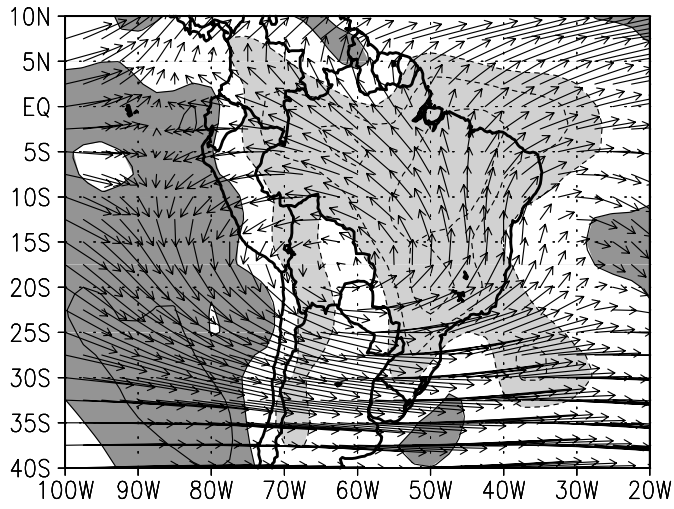
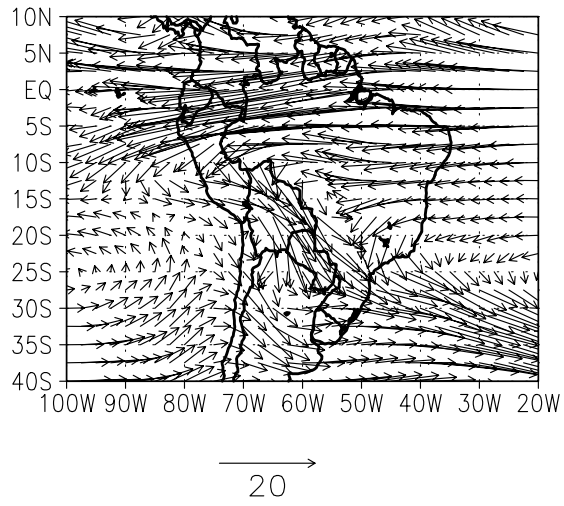


FIGURE 2

→  
20

a) 1998



b) 1999

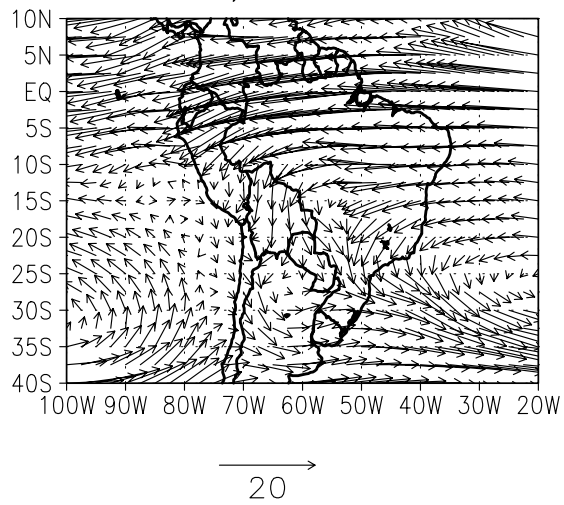


FIGURE 3

a) JFM 1998 (total=44, TROPICS=10, SACZ=8, SSA=26)

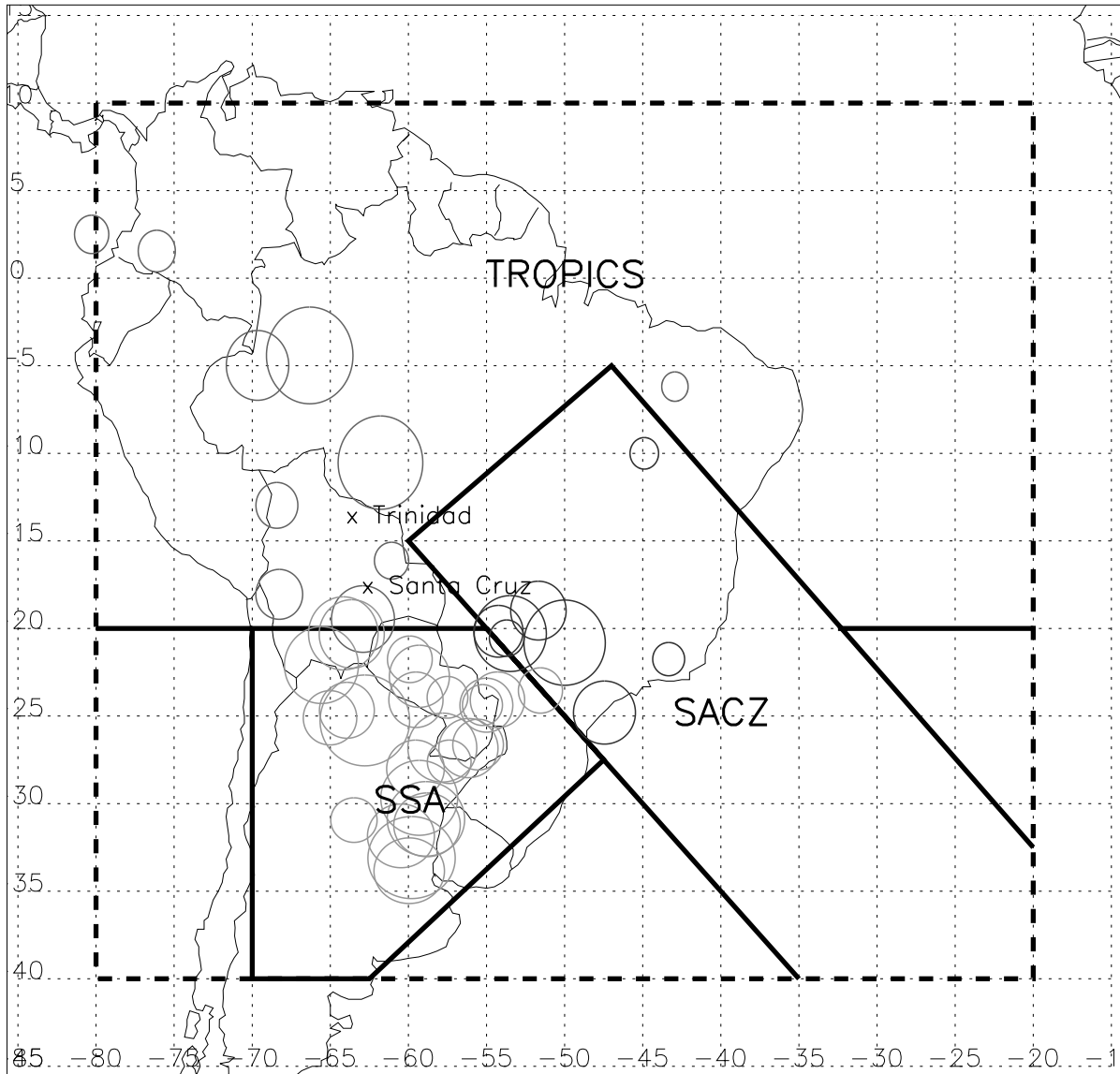


FIGURE 4

b) JFM 1999 (total=91, TROPICS=56, SACZ=16, SSA=17)

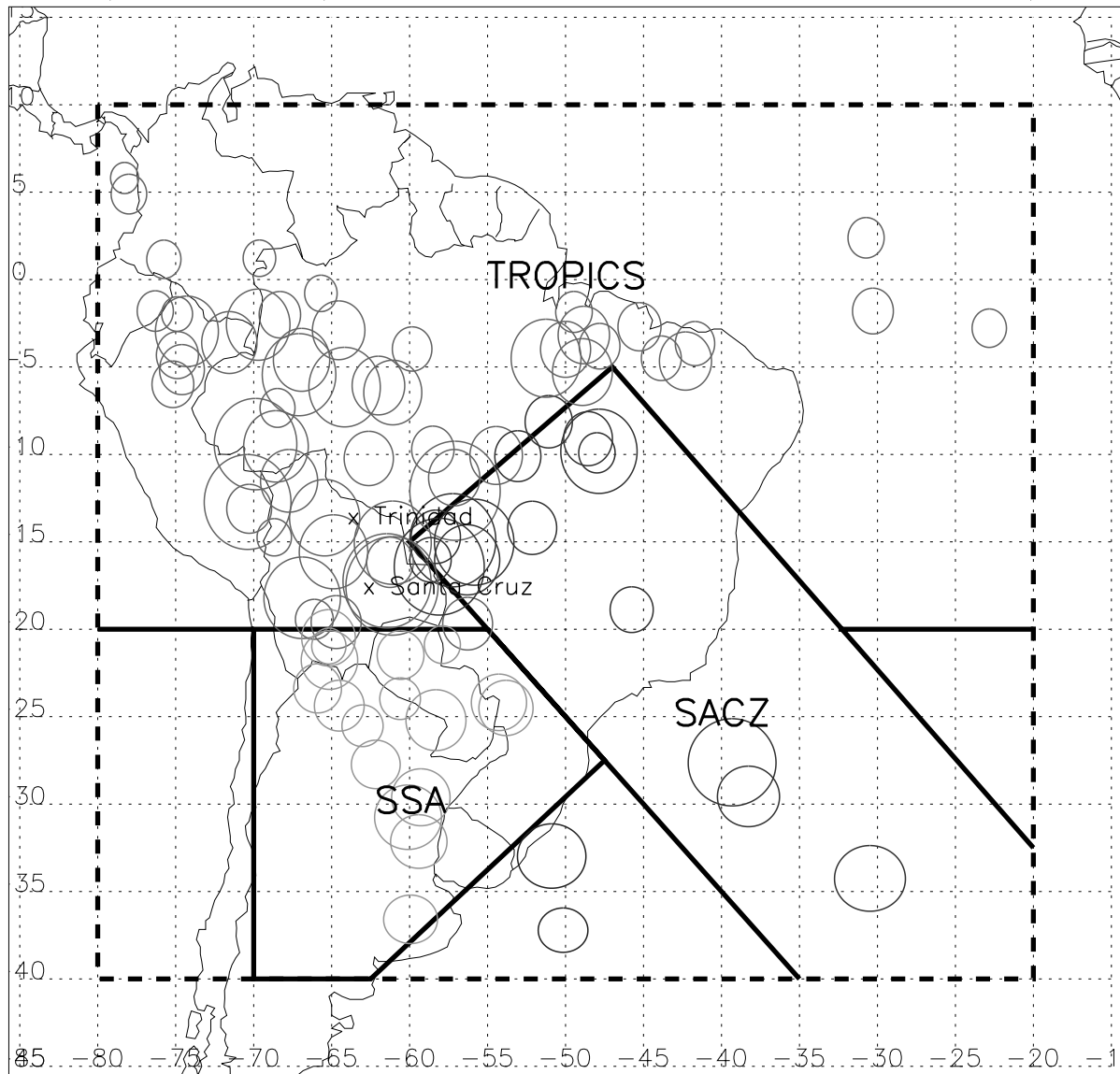


FIGURE 4

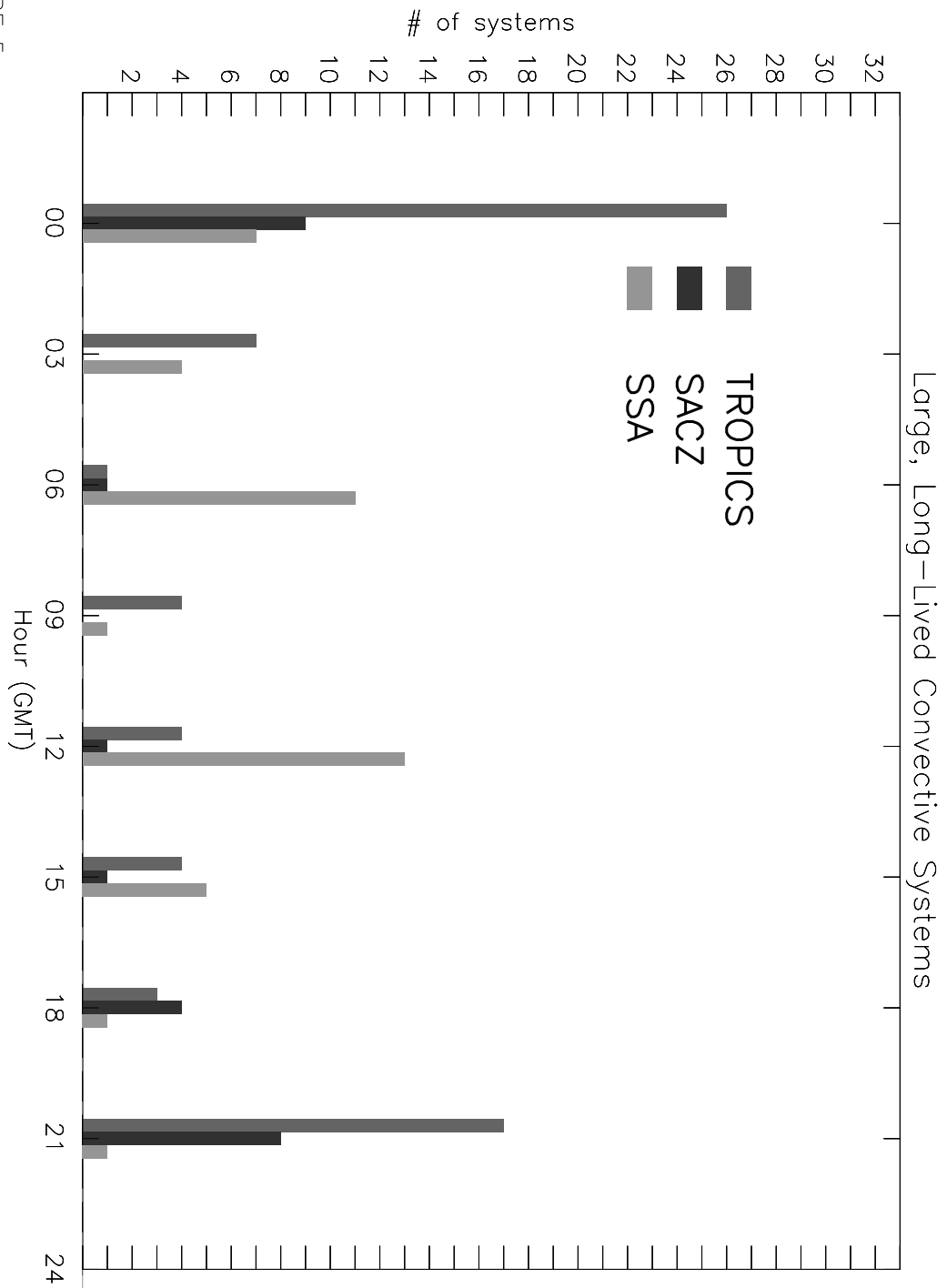


FIGURE 5

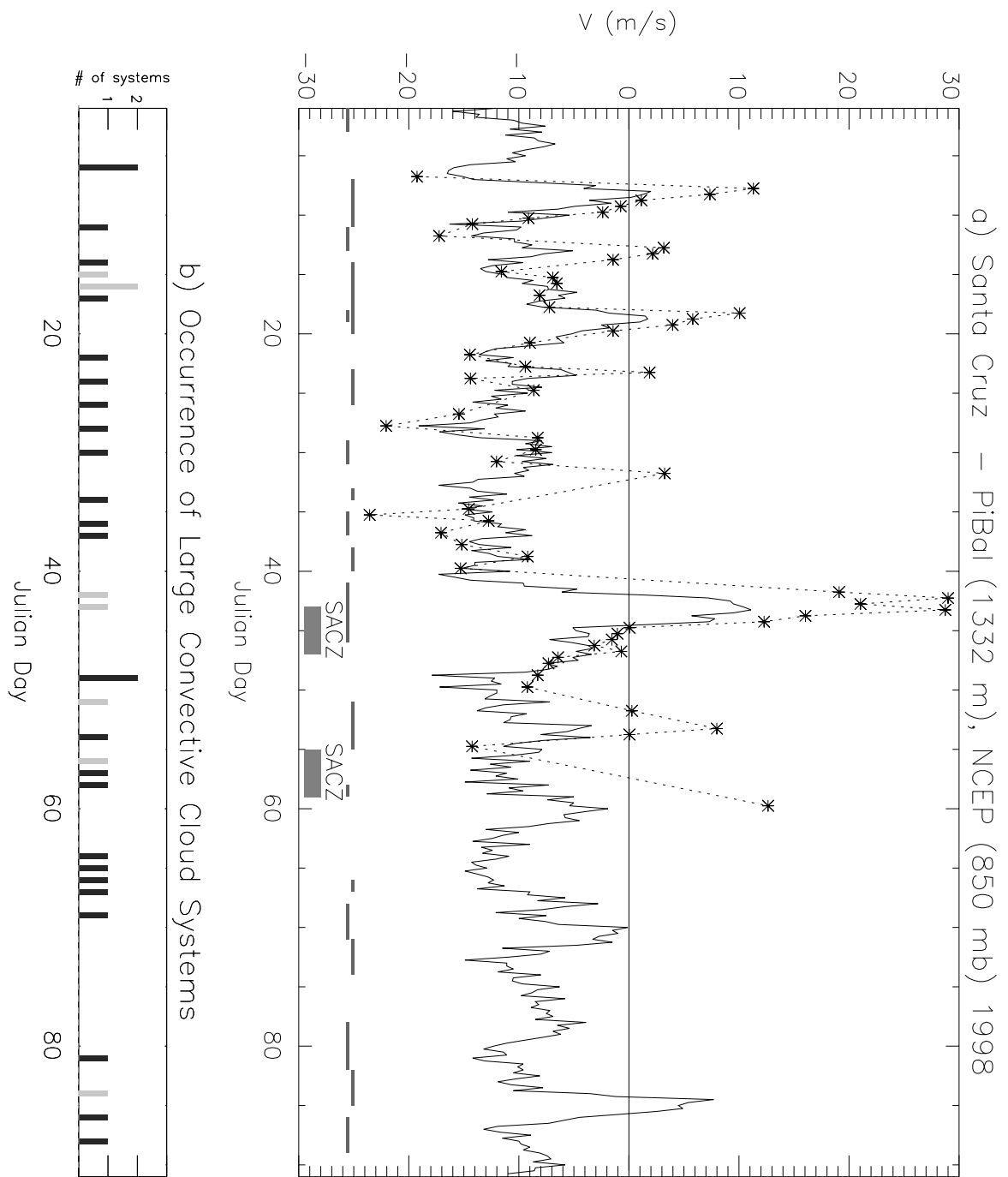


FIGURE 6

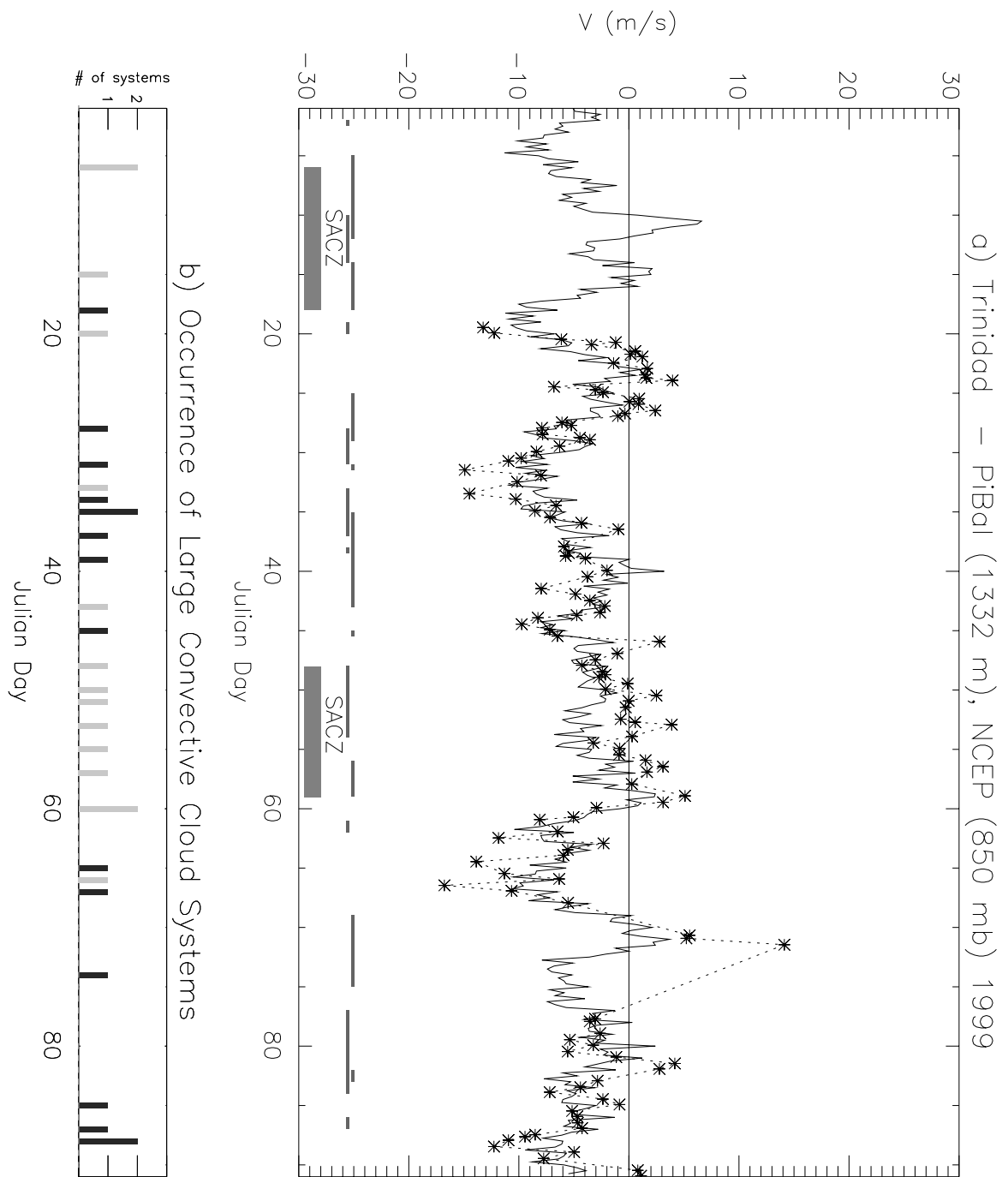


FIGURE 7